15 GHz Monitoring of Gamma-ray Blazars with the OVRO 40 Meter Telescope in Support of *Fermi*

J. L. Richards, W. Max-Moerbeck, V. Pavlidou, T. J. Pearson, A. C. S. Readhead, and M. A. Stevenson
California Institute of Technology, Owens Valley Radio Observatory, Pasadena, CA 91125, USA
S. E. Healey, R. W. Romani, and M. S. Shaw
Department of Physics/KIPAC, Stanford University, Stanford, CA 94305, USA
L. Fuhrmann, E. Angelakis, and J. A. Zensus
Max-Planck-Institut-für-Radioastronomie, Bonn 53121, Germany
K. Grainge
Astrophysics Group, Cavendish Laboratory, University of Cambridge, Cambridge, UK
G. B. Taylor
Department of Physics and Astronomy, University of New Mexico, Albuquerque, NM 87131, USA

We present results from the first two years of our fast-cadence 15 GHz gamma-ray blazar monitoring program, part of the F-GAMMA radio monitoring project. Our sample includes the 1158 blazars north of $-20°$ declination from the Candidate Gamma-Ray Blazar Survey (CGRaBS), which encompasses a significant fraction of the extragalactic sources detected by the *Fermi* Gamma-ray Space Telescope. We introduce a novel likelihood analysis for computing a time series variability amplitude statistic that separates intrinsic variability from measurement noise and produces a quantitative error estimate. We use this method to characterize our radio light curves. We also present results indicating a statistically significant correlation between simultaneous average 15 GHz radio flux density and gamma-ray photon flux.

1. INTRODUCTION

The extragalactic gamma-ray sky is dominated by blazars, a class of active galactic nuclei (AGN) that exhibit powerful, variable broadband emission, likely due to observing a relativistic jet aimed close to the line of sight. Despite intensive study and modeling, the mechanisms that generate the prodigious emission in these objects are not well constrained. Because of the broadband emission, simultaneous multi-wavelength studies provide powerful probes of the structures and processes that give rise to the blazar phenomena.

The Large Area Telescope (LAT) on the *Fermi* Gamma-ray Space Telescope (GST) provides unprecedented all-sky gamma-ray monitoring, and detected 104 bright AGN with radio counterparts in its first three months of operation and will likely detect many more as its mission continues [Abdo *et al.* 2009]. This offers the opportunity to perform simultaneous multi-wavelength studies of statistically large numbers of sources. Simultaneity of measurements is important to eliminate ambiguities arising from variability. Using statistically large samples is also extremely important—although AGN exhibit many common features, they make up a complex taxonomy and it is difficult to extrapolate features from a small sample to AGN as a whole.

Correlating gamma-ray emission with activity at radio wavelengths can provide a powerful probe of blazar physics. Through high-resolution VLBI, radio observations are uniquely capable of spatially resolving AGN and identifying the location of emission within the structure. If emission events at other wavelengths can be connected with events in radio, their emission locations can perhaps be identified. This is extremely important to help constrain models of the emission and eventually reach a full understanding of the AGN phenomena.

1.1. OVRO 40 M Monitoring Program

Since 2007, we have carried out 15 GHz observations of the 1158 sources north of $-20°$ declination in the Candidate Gamma-Ray Blazar Survey (CGRaBS) sample with the Owens Valley Radio Observatory (OVRO) 40 M Telescope.[1] The CGRaBS are a sample of 1625 sources, mostly blazars, selected by their flat radio spectra and X-ray fluxes to resemble the blazars detected by EGRET [Healey *et al.* 2008]. These were expected to constitute a large sample of the extragalactic sources detected by *Fermi*. Each source is observed approximately twice per week with a thermal noise floor of about 5 mJy. In addition to the CGRaBS core sample, AGN detected by *Fermi* are regularly added to our program if they are found to be detectable with our sensitivity.

1.2. The F-GAMMA Project

The OVRO 40 M program is a key component of the *Fermi*-GST Multi-wavelength Monitoring Al-

[1] Data from the OVRO 40 M monitoring program are available from `http://www.astro.caltech.edu/ovroblazars`.

liance (F-GAMMA) project [Angelakis *et al.* 2008, Fuhrmann *et al.* 2007]. Also within the F-GAMMA project, spectra of a smaller sample of about 60 bright sources, selected *ad hoc* based on historically interesting behavior, are monitored monthly at twelve frequencies between 2.7 and 270 GHz using the Effelsberg 100 m and Pico Veleta 30 m telescopes. The coordinated F-GAMMA monitoring strategy provides both broad spectral monitoring of a moderate number of sources, as well as high-cadence monitoring of a very large, statistically well-defined sample well-suited for population studies.

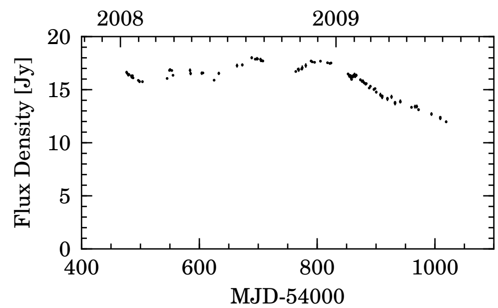

Figure 1: OVRO 15 GHz light curve for 3C 279.

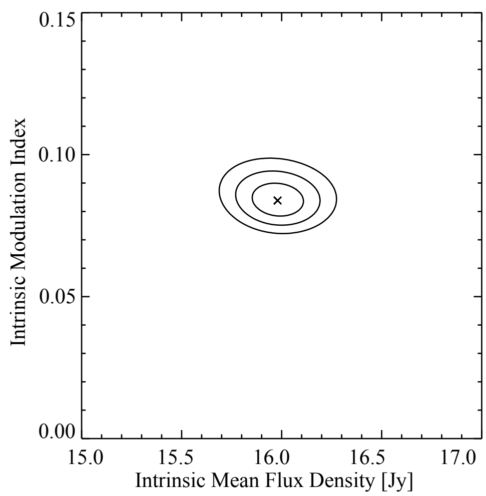

Figure 2: Maximum likelihood and 1, 2, and 3σ contours for 3C 279.

2. QUANTIFYING VARIABILITY

A number of measures of the time-independent variability amplitude of a light curve are used in the AGN literature, such as the variability index [e.g. Aller *et al.* 1992] and the modulation index [e.g. Fuhrmann *et al.* 2008]. In general, these methods produce a number that quantifies the amplitude of variations in the source but do not produce an estimate of the uncertainty in this number. Furthermore, measurement errors in the data, if considered at all, are not handled in a sophisticated way. Finally, some of these methods suffer from pathological failures that complicate interpretation. For example, in the presence of high noise, the variability index can yield negative indices that must be rejected.

2.1. The Intrinsic Modulation Index

To address these issues, we introduce the *intrinsic modulation index* defined as $\hat{m} = \sigma_0/S_0$. Here S_0 and σ_0 are the intrinsic mean and standard deviations of the source flux density time series. By "intrinsic" we mean excluding contributions from errors in the measurement process.[2]

Of course these intrinsic quantities are unknown, so we have developed a likelihood method for estimating $\hat{m}$ from a measured light curve and its associated measurement errors. For this method, we postulate a parametric model for the intrinsic distribution of flux densities from the source. Here we assume a Gaussian distribution parameterized by its mean (S_0) and intrinsic modulation index ($\hat{m}$, a convenient rescaling of the standard deviation). This choice of distribution is not unique, and in fact is clearly not the best description for many sources. However, it is analytically convenient and comparisons with other distributions suggest that the errors that result are tolerable.

Given a collection of flux densities and estimated measurement uncertainties from a light curve (Figure 1), we compute the maximum joint likelihood of S_0 and $\hat{m}$ and find the isolikelihood contours representing 1, 2, and 3σ (68.3%, 95.5%, and 99.7%) confidences (Figure 2). We then marginalize over S_0 to produce a likelihood distribution in $\hat{m}$ (Figure 3). The peak of this distribution gives our estimate for $\hat{m}$, and its width gives the uncertainty (which is, in general, asymmetric). The uncertainty includes the contribution of measurement uncertainties, as well as effects of a limited number of observations. This method agrees with the standard modulation index, as shown in Figure 4, which is reassuring.

2.2. Population Studies

Armed with the intrinsic modulation index, we can compare the variability amplitudes between subpopulations of our sample. Again using a likelihood analysis we model each subpopulation with a distribution (here we show an example using a Gaussian distri-

[2]This should not be confused with "intrinsic behavior" of an astronomical source—our method does not, for example, separate variability due to interstellar scintillation from variability in the source itself.

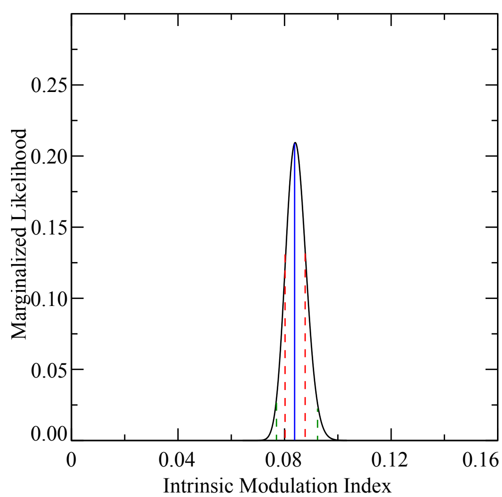

Figure 3: Marginalized likelihood distribution for the intrinsic modulation index for 3C 279. Vertical lines indicate maximum likelihood value (sold) and ± 1 and $\pm 2\sigma$ intervals (dashed).

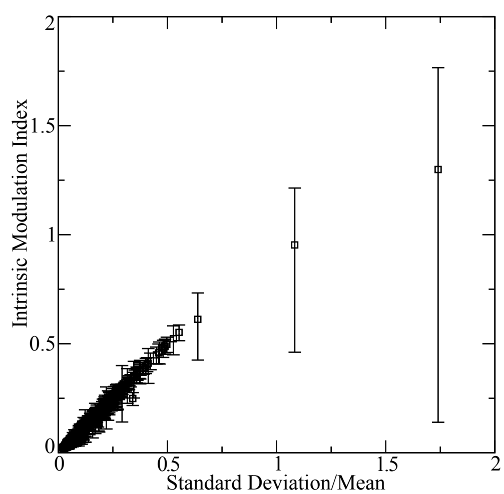

Figure 4: Intrinsic modulation index for OVRO CGRaBS sample plotted against the traditional modulation index.

bution) in intrinsic modulation index with mean m_0 and standard deviation σ_0. Figure 5 shows the 1, 2, and 3σ isolikelihood contours for a random split of our population—as expected, these subpopulations overlap significantly in parameter space. This likelihood method permits two-dimensional discrimination between population parameters, giving the capability to find differences between populations with distributions that overlap significantly in either parameter individually.

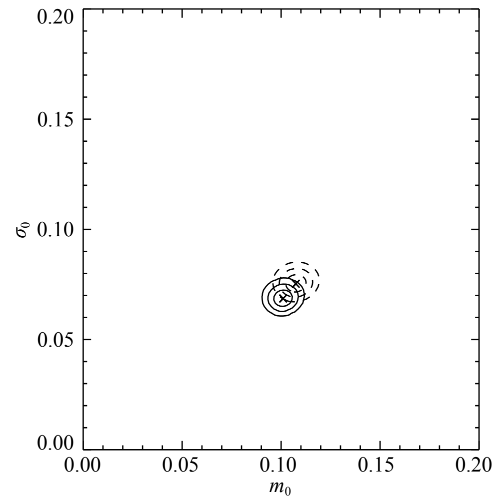

Figure 5: Likelihood contours for variability parameters of randomly split OVRO CGRaBS sample.

3. RADIO-GAMMA CONNECTION

A connection between radio and gamma-ray emission, manifested in a correlation between flux densities in the two bands, would be important evidence for common emission origins. In the EGRET era, some evidence for such a connection was found, but could not be convincingly demonstrated to reflect an intrinsic correlation in source luminosities [Mücke *et al.* 1997]. A number of red shift and sample selection effects can work to induce an apparent correlation. Recently, Kovalev *et al.* [2009] found an apparent correlation of *Fermi* gamma-ray photon fluxes with quasi-simultaneous 15 GHz VLBI core flux densities. However, the question as to whether this apparent correlation is significant in the face of biases still stands.

3.1. Significance: Likelihood Method

We have developed a Monte Carlo method for evaluating the significance of apparent correlations that accounts for both red shift and selection effects and is compatible with sample selection methods that cannot be quantified or reproduced. Our method uses randomly-paired luminosities and red shifts from the true data set to construct a comparison sample with no intrinsic correlations. By constructing many such samples, the probability density for chance correlations can be estimated and used to evaluate the significance of the observed correlation.

It should be noted that although this method can eliminate selection effects when evaluating the significance of a correlation, it cannot generalize a conclusion about the existence of a correlation outside the sample being tested. To make claims about, say, the general blazar population, a representative subsample of that population is still required.

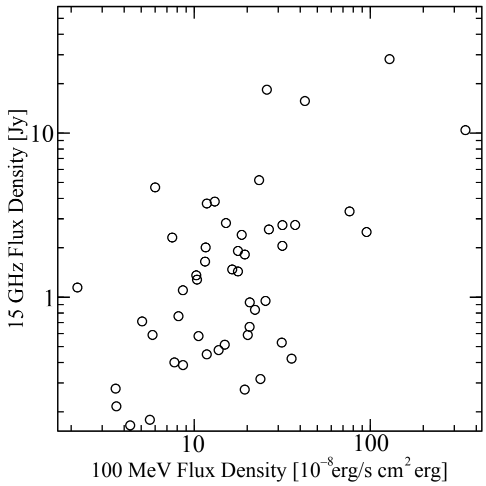

Figure 6: OVRO 15 GHz flux density versus *Fermi*-LAT 100 MeV flux density.

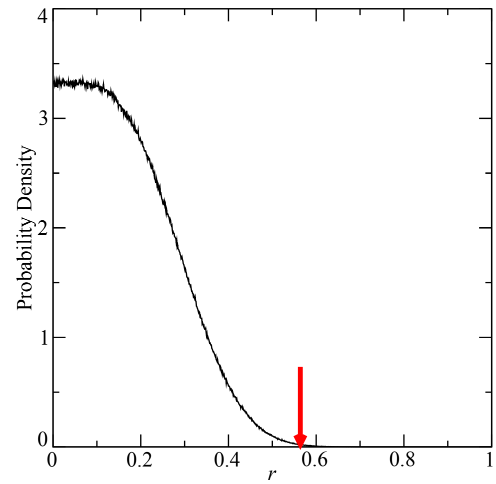

Figure 7: Monte Carlo-estimated probability density function for the correlation coefficient, r, between OVRO 15 GHz and *Fermi* 100 MeV flux densities. Arrow indicates measured value.

3.2. Results

There are 49 sources with known redshifts in both the OVRO CGRaBS sample and the *Fermi*-LAT 3-month bright AGN list [Abdo *et al.* 2009]. Simultaneous time average 15 GHz radio and 100 MeV *Fermi* gamma-ray flux densities for each of these sources are shown in Figure 6. These data are averaged over the first three months of *Fermi* operation, August 4–October 30, 2008. A correlation is visually apparent, and the Pearson product-moment correlation coefficient for these data is $r = 0.56$. Is this a significant correlation?

Applying our Monte Carlo method to the OVRO 15 GHz data, we obtain the estimated probability density function shown in Figure 7. We find a probability of about $P = 5 \times 10^{-4}$ to find as large or larger a correlation by chance. Using multifrequency data from the F-GAMMA project for a somewhat smaller population of sources we find a stronger correlation ($r = 0.89$, $P = 4 \times 10^{-5}$) at 140 GHz and a decrease in both correlation coefficient and significance as the radio frequency decreases. There is good agreement between the Effelsberg 14.6 GHz result and the OVRO 15 GHz result, although the OVRO result is more significant due to its larger sample size. Correlation results at all frequencies are given in Table I.

Table I Radio-Gamma-ray Flux-Flux Correlation Results

Frequency [GHz]	**Correlation Coefficient**	**Chance Probability**	**Site**[a]
142	0.89	4×10^{-5}	PV
86	0.86	2×10^{-5}	PV
43	0.83	7×10^{-4}	EFF
32	0.74	6×10^{-4}	EFF
22	0.59	0.01	EFF
15	0.56	5×10^{-4}	OVRO
14.6	0.49	0.03	EFF
10.5	0.43	0.05	EFF
8.4	0.40	0.06	EFF
4.8	0.40	0.08	EFF
2.6	0.43	0.06	EFF

[a]Site legend: PV=Pico Veleta IRAM 30 m; EFF=Effelsberg 100 m; OVRO=OVRO 40 m.

4. CONCLUSIONS

Densely-sampled light curves for the 1158 northern CGRaBS and a number of other sources have been collected using the OVRO 40 M Telescope since 2007. In addition, monthly radio spectra of about 60 sources have been collected through the F-GAMMA project. Work is underway to combine these radio light curves with gamma-ray data from the *Fermi*-GST.

We have developed a new likelihood method, the intrinsic modulation index, for quantifying the degree of variability in a light curve. Unlike standard measures, our method quantifies the uncertainty in its output after accounting for measurement errors, and can be used to compare data sets that are inhomogeneous with respect to measurement errors or number of measurements.

Finally, we conclude that we have found clear evidence for a statistically significant correlation between OVRO and F-GAMMA radio and *Fermi*-LAT gamma-ray flux densities. Using our Monte Carlo method, we have demonstrated that this correlation is not the result of red shift or selection effects. Our method can be applied to samples, such as the F-

GAMMA sample, that were not selected using statistical criteria. This correlation is strongest and most significant at higher radio frequencies, but is still highly significant at least as low as 15 GHz.

Acknowledgments

The OVRO 40 M program is supported in part by NASA grant NNX08AW31G and NSF grant AST-0808050. WM acknowledges support from the U.S. Department of State and the Comisión Nacional de Investigación Científica y Tecnologica (CONICYT) in Chile for a Fulbright-CONICYT scholarship. VP acknowledges support for this work provided by NASA through Einstein Postdoctoral Fellowship grant number PF8-90060 awarded by the Chandra X-ray Center, which is operated by the Smithsonian Astrophysical Observatory for NASA under contract NAS8-03060.

References

Abdo, A. A., M. Ackermann, M. Ajello, W. B. Atwood, M. Axelsson, L. Baldini, J. Ballet, G. Barbiellini, D. Bastieri, B. M. Baughman, K. Bechtol, R. Bellazzini, *et al.*, 2009, Astrophysical Journal **700**, 597.

Aller, M. F., H. D. Aller, and P. A. Hughes, 1992, Astrophysical Journal **399**, 16.

Angelakis, E., L. Fuhrmann, N. Marchili, T. P. Krichbaum, and J. A. Zensus, 2008, Memorie della Societa Astronomica Italiana **79**, 1042.

Fuhrmann, L., T. P. Krichbaum, A. Witzel, A. Kraus, S. Britzen, S. Bernhart, C. M. V. Impellizzeri, I. Agudo, J. Klare, B. W. Sohn, E. Angelakis, U. Bach, *et al.*, 2008, Astronomy and Astrophysics **490**, 1019.

Fuhrmann, L., J. A. Zensus, T. P. Krichbaum, E. Angelakis, and A. C. S. Readhead, 2007, in *The First GLAST Symposium*, edited by S. Ritz, P. Michelson, and C. A. Meegan (Stanford University, Stanford, CA), volume 921 of *AIP Conference Proceedings*, pp. 249–251.

Healey, S. E., R. W. Romani, G. Cotter, P. F. Michelson, E. F. Schlafly, A. C. S. Readhead, P. Giommi, S. Chaty, I. A. Grenier, and L. C. Weintraub, 2008, Astrophysical Journal **175**, 97.

Kovalev, Y. Y., H. D. Aller, M. F. Aller, D. C. Homan, M. Kadler, K. I. Kellermann, Y. A. Kovalev, M. L. Lister, M. J. McCormick, A. B. Pushkarev, E. Ros, and J. A. Zensus, 2009, Astrophysical Journal **696**, L17.

Mücke, A., M. Pohl, P. Reich, W. Reich, R. Schlickeiser, C. E. Fichtel, R. C. Hartman, G. Kanbach, D. A. Kniffen, H. A. Mayer-Hasselwander, M. Merck, P. F. Michelson, *et al.*, 1997, Astronomy and Astrophysics **320**, 33.